



HAL
open science

Measurement of the water vapour permeability of earth plasters using small-scale wind tunnels under variable air flow regimes

Fionn McGregor, T. Mauffré, M.-S. Force, E. Contraires, A. Fabbri

► To cite this version:

Fionn McGregor, T. Mauffré, M.-S. Force, E. Contraires, A. Fabbri. Measurement of the water vapour permeability of earth plasters using small-scale wind tunnels under variable air flow regimes. *Materials and structures*, 2022, 55 (4), pp.110. 10.1617/s11527-022-01950-8 . hal-04111687

HAL Id: hal-04111687

<https://univ-pau.hal.science/hal-04111687>

Submitted on 31 May 2023

HAL is a multi-disciplinary open access archive for the deposit and dissemination of scientific research documents, whether they are published or not. The documents may come from teaching and research institutions in France or abroad, or from public or private research centers.

L'archive ouverte pluridisciplinaire **HAL**, est destinée au dépôt et à la diffusion de documents scientifiques de niveau recherche, publiés ou non, émanant des établissements d'enseignement et de recherche français ou étrangers, des laboratoires publics ou privés.



Measurement of the water vapour permeability of earth plasters using small-scale wind tunnels under variable air flow regimes

F. McGregor · T. Mauffré · M.-S. Force · E. Contraires · A. Fabbri

Received: 17 December 2021 / Accepted: 25 March 2022 / Published online: 16 April 2022
© RILEM 2022

Abstract To determine the water vapour permeability of porous building materials, the wet cup and dry cup tests are frequently performed. Those tests have shown to present high discrepancy. The water vapour permeability of building materials is an essential parameter to determine the hygrothermal behaviour of the material and its impact on indoor comfort. Several previous studies have aimed to improve the reproducibility of the tests, by improving the protocol, the analysis of the results, notably by taking into account the surface film resistance. Yet, it is commonly accepted with no evidence that this surface film resistance can be neglected for an air velocity above 2 m/s over the cup. This study aims at experimentally testing the influence of either the flow regime or the flow velocity on the robustness of the measured water vapour permeability. For this purpose, two mini wind tunnels were designed to produce a laminar or a turbulent flow above the cups with variable air

velocity. Water vapour permeability tests were performed in the tunnels with varying air velocity and flow regime on earth plasters with different compositions. The results have shown that regardless of the air velocity and flow regime, the surface film resistance should not be neglected. Based on the presented results, to reach an optimal repeatability, the use of wind tunnels should be considered as they allow to precisely control the air flow above the samples.

Keywords Earthen materials · Water vapour permeability · Small low speed wind tunnels · Surface resistance factor · Wet-cup experiments · Earth plasters

1 Introduction

Local natural building materials such as raw earth or biobased building materials are gaining visibility because of their low environmental impact [1, 2]. Earth as a building material is relevant due to its high availability [3] and the potential to be used as a structural and load bearing material [4, 5]. Many research papers also suggest that earth has a positive impact on indoor environments. Actually, comfort experienced in dwellings is impacted by both temperature and humidity [6]. Thus, through their passive moisture regulation potential [7–9] earthen materials

F. McGregor (✉)
Université de Pau et des Pays de l'Adour, E2S UPPA,
SIAME, Anglet, France
e-mail: fionn.mcgregor@univ-pau.fr

T. Mauffré · M.-S. Force · A. Fabbri
GCD-LTDS, UMR 5513 CNRS, ENTPE, 3 Rue Maurice
Audin, 69120 Vaulx-en-Velin, France

E. Contraires
TPCDI-LTDS, UMR 5513 CNRS, Ecole Centrale de
Lyon, 36 Avenue Guy de Collongue, 69134 Écully,
France



can improve indoor comfort while reducing energy consumed via HVAC systems [10, 11].

Numerous studies have been dedicated to the simulation of hygrothermal couplings in construction materials (for example [12, 13]). It led to the development of numerous models at several levels of complexity. The Glaser method, for example, which is classically used to assess the risk of condensation, is based on a permanent state assumption and do not take into account water sorption processes, while other models, rather dedicated to precisely quantify heat and mass couplings, take into account differences between vapour adsorption and desorption process [14] or even introduce local non-equilibrium conditions [15]. Anyway, despite their differences, all these models are based on heat and mass balance equation, and their accuracy strongly depends on the quality of some key input parameters like the intrinsic water vapour permeability [16]. This latter is commonly determined through wet cup and dry cup tests. Even if they are standardized tests [17], they commonly lead to poorly reliable results on hygroscopic building materials like raw earth or biobased building materials. This issue was underlined by round robin campaigns which gave errors of up to 45% for the dry cup test and 43% for the wet cup test [18] for the same material. According to [19], the most important tests parameters influencing the repeatability of the cup method are the thickness of the material, the sealing method and the boundary conditions. By fixing them and by imposing an increased air velocity above the samples they managed to reduce errors down to 10% and 14% respectively for the dry cup and the wet cup test [19]. Pazera and Salomvaara [20] also investigated humidity boundary conditions generated by different salts and desiccants. The 0% RH condition is for example an unrealistic value as the measured values show a rapid increase, in less than 24 h those reach up to 10% RH [20]. Previous studies, [21, 22] have shown the importance of the thickness on the measured results for a same material. It was concluded that the cup tests do not give directly the intrinsic vapour permeability of the material, but always an apparent permeability which is a combination of surface and material properties. A reduction of the material's thickness leads to a reduced resistance to vapour diffusion, but external surface resistance to vapour diffusion will remain unchanged, if no correction is applied this consequently leads to a variation of the calculated vapour permeability. To avoid this

issue, the ISO standard [17] recommends sufficiently thick materials and an air velocity of at least 2 m/s above the samples for very permeable materials. However, this recommendation seems to be difficult to achieve, and may not be sufficient for high permeable materials, previous research suggests that the air velocity continues to impact results even for a ventilation speed above 2 m/s [21]. Furthermore, some authors underlined the technical difficult to effectively control this parameter, especially in climatic chambers [21]. Finally, the flow regime (i.e. laminar or turbulent) is known to influence mass transfer surface coefficient, while it is hardly controllable in set-ups commonly used for dry and wet cups experiments [23]. In this context, this paper investigates the influence of different air velocities and flow regimes on the vapour permeability tests of earth plasters. Two different small low speed wind tunnels are developed to establish controlled conditions above the test cups. One wind tunnel has been designed to maintain a laminar flow, while the second one remains in the turbulent regime. The air velocities are set to constant values of approximately 1, 2 and 3 m/s. Results are analysed regarding the correction proposed in previous studies [21, 22] and lead to some propositions to increase the robustness of water vapour permeability tests.

2 Materials and methods

2.1 Description of the earth plasters used

Based on classical recommendation for the soil/sand mix for earth plasters, sample compositions were designed in order to be sufficiently representative of a real earth plaster [24], using variable granulometry of siliceous sand and earth content.

The soil was taken from an existing rammed earth construction located in Dagneux in the “Auvergne-Rhône-Alpes” region in the South-East of France. It was sieved to a very fine fraction of 60 μm . The resulting material, composed of around 26% of clay size fraction (below 2 μm), is denoted by “earth” in the rest of this paper. Based on a semi-quantitative analysis realised by the ERM laboratory in France (Poitiers), the clay fractions is composed of stratified Illite/smectite (17% of total earth) swelling clays and of Kaolinite (9% of total earth).



Sample's manufacture was described in detail in [25]. Sand and earth were mixed in a dry state, then an adequate quantity of water was added, this quantity was previously determined to achieve correct workability for plasters. In type A samples, the same sand/earth ratio was kept constant, but with variable sand particle sizes. On the opposite, type B samples have the same sand particle size but variable sand/earth ratios. Main characteristics of the earth plasters formulations are summarised in Table 1.

Samples were cast in a cylindrical mold of 7 cm in diameter and 2 cm in height. They were kept at least two weeks in a controlled temperature and humidity environment (20 °C, 50%HR) before being tested.

2.2 Water vapour permeability measurement

2.2.1 Experimental procedure

Water vapour permeability tests were realised following the wet cup protocol described in the ISO standard [17]. Polymethyl methacrylate cups of outer diameter corresponding to the sample size were used. The samples were sealed to the cup using silicone and aluminium tape. The vapour pressure gradient through the sample was generated by setting the RH at 50% (denoted by φ_r) and the temperature at 20 °C in a controlled room and a relative humidity of $\varphi_c = 75\%$ in the cup by a corresponding saturated salt solution of NaCl. These humidity conditions were chosen according to the materials' water content variation towards relative humidity. According to the adsorption/desorption curves, those relative humidities correspond to the region where the variation trend remains linear, and thus it avoids generating important water content gradients through the samples.

2.2.2 Applied corrections

The measurement during the wet cup test gives a variation of mass per time. Its linear correlation gives the slope G :

$$G = \frac{dm}{dt} \quad (1)$$

To obtain the apparent vapour permeability of the material (denoted by δ_p), the slope is corrected by the surface area of the sample exposed (denoted by A) and the vapour pressure gradient (equal to $\Delta p_v/d_m$, where $\Delta p_v = (\varphi_c - \varphi_r)p_v^{sat}$, with $p_v^{sat} = 2340$ Pa the vapour pressure at saturation at 20 °C and d_m the thickness of the sample):

$$\delta_p = \frac{G d_m}{A \Delta P_v} \quad (2)$$

This apparent water vapour permeability, as described in [21, 22] and illustrated in the Fig. 1, theoretically includes the resistance to diffusion by the air layer in the cup Z_a , the resistance due to the actual material itself Z_m and the resistance to diffusion of a still layer at the surface of the material Z_s . So that the apparent moisture resistance which is measured, denoted by Z^* , is actually equal to:

$$Z^* = \frac{d_m}{\delta_p} = Z_m + Z_a + Z_s \quad (3)$$

with

$$Z_a = \frac{d_a}{\delta_a} ; Z_m = \frac{d_m}{\delta_{p,c}} ; Z_s = \frac{1}{\beta} \quad (4)$$

where d_a is the thickness of the air layer within the cup, δ_a is the free diffusion vapour coefficient in air, β is the surface vapour exchange coefficient and $\delta_{p,c}$ is the effective water vapor permeability of the material, which thus writes in the form:

Table 1 Characteristics of the earth plaster samples

Samples	Sand particle size	Earth (%)	Sand (%)	Average apparent density (g/cm ³)
A1	0–315 μm	83	17	1.69
A3	315–630 μm	83	17	1.62
A9	0–2 mm	83	17	1.87
B1	0–630 μm	70	30	1.87
B3	0–630 μm	60	40	1.89

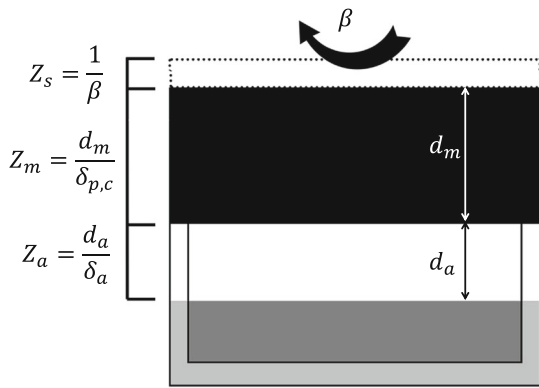


Fig. 1 Resistance to water vapour diffusion in the wet cup assembly

$$\delta_{p,c} = \frac{d_m}{Z_m} = \frac{G d}{A \Delta p_v - G(Z_a + Z_s)} \quad (5)$$

In [21], they conclude that the value of Z_s is quite difficult to predict, especially for highly permeable materials, and thus that additional measurements are needed to estimate its value. This was confirmed by [22].

This estimation was done in previous studies [21, 22, 26], the principle of this correction is illustrated in Fig. 2. At least three thicknesses need to be measured to determine Z_s which is then obtained through the regression line on the $\frac{d_m}{\delta_p^{ISO}}$ versus d_m plot. In

this case, δ_p^{ISO} , is the apparent water vapour permeability without the resistance of the air layer in the cup:

$$\delta_p^{ISO} = \frac{G d_m}{A \Delta p_v - G Z_a} \quad (6)$$

Therefore, the origin of the regression line illustrated in Fig. 2 when the material thickness approaches zero represents the remaining surface film resistance Z_s .

3 Design of the small low speed wind tunnels (SLSWT)

To control the air flow regime over the water vapour permeability test cups, two SLSWT were designed. The first wind tunnel aims at providing turbulent conditions quite similar to those that should be reached in a ventilated box or climatic chamber yet with homogeneous and repeatable conditions for each sample. The second one aims at reaching a laminar flow over the cups. Those two types of tunnels were used to compare the impact of different flow regimes on the surface film resistance. The size of the tunnels were chosen to at least be able to measure three small cups. The ventilation was insured by a 12 cm fan and the structural elements of the tunnels were made of foam board.

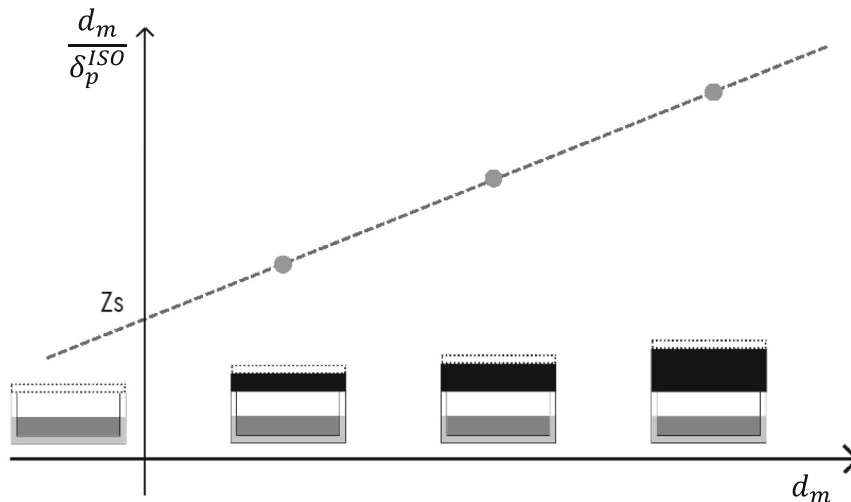


Fig. 2 The principle for the measure of the surface film resistance, Z_s . The tested sample is represented in black, the air layer in white, the saline solution in grey and the zone within the dotted lines corresponds to the surface film



3.1 Turbulent wind tunnel

The schematic design of the tunnel is shown in Fig. 3. It is composed by three parts: chamber test, contraction area and ventilation zone. The contraction area was designed in order to reach homogeneous air velocities of 1 m/s, 2 m/s and 3 m/s within the test chamber. It is usually considered that for a flow in a circular or rectangular duct a Reynolds number below 2000 indicates a laminar flow and above 4000 a turbulent regime, the range between 2000 and 4000 corresponds to a transition [27]. In consequence, the geometry of the test chamber was designed in order to obtain a Reynolds' number higher than 4000 whatever the tested ventilation speed, that are 1 m/s, 2 m/s and 3 m/s. For that purpose, Reynolds number was calculated based on Eq. 7 for air velocities.

$$Re = \frac{U \cdot D_h}{\nu_c} \tag{7}$$

where U is the air velocity measured in the tunnel, D_h is the hydraulic diameter and ν_c is the kinematic velocity of air. The hydraulic diameter of a rectangular section is calculated as:

$$D_h = \frac{2ab}{a+b} \tag{8}$$

where a is the height of the chamber test and b its width.

In addition, in order to avoid edge effects, the contact zone between the air flow and the sample should be spaced out of a length δ from the walls of the tunnel. According to [27], δ can be approximated by the relation:

$$\delta \approx \frac{b}{\sqrt{Re}} \tag{9}$$

Given all these constrains, values of $a = 5$ cm and $b = 15$ cm were chosen. They lead to Reynolds numbers given in Table 2.

Finally, a distance of $L_c = 30$ cm between the end of the contraction area and the first cup was set in order to allow the stabilization of the air flow in the test chamber. According to the common dynamic set-up length formulae, this value might appear a bit small for the highest air velocities reached in this study. However, for practical reasons, it was not possible to exceed this length, and the effective relative homogeneity of the air was successfully post-evaluated.

3.2 Laminar wind tunnel

The tunnel is composed by five parts: settling chamber, contraction zone, test chamber, diffuser and ventilation zone (cf. Fig. 4). The honeycomb was 3D printed, while the screen structure was made of a perforated thin board. To achieve a correct laminar flow, the size and air entry into the tunnel was design accordingly to the recommendations given in [28, 29]. Values obtained for the main characteristics are given in Table 3. For practical reasons, the contraction design was not able to match perfectly the curvature shape following the equation given by Bell and Metha [28]. The nozzle shape was approached by discretization so that slope drops were lower than 30° in order to avoid a local flow deflection. The laminar regime and the effective homogeneity of the flow were also successfully post-evaluated.

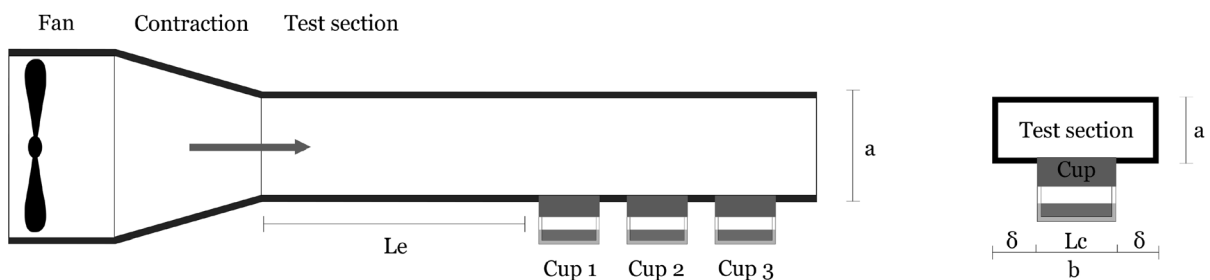


Fig. 3 Schematic representation of the turbulent SLSWT



3.3 Air velocity and flow regime in the wind tunnels

An experimental campaign has been realised in order to test that the SLSWT were functioning properly. At first, the flow regime was checked through a visualisation test. For that purpose, small strings were attached to a net in the section of the tunnel (cf. Fig. 5). The movement of these strings (or tufts) should depend on the nature of the flow regime. The turbulent regime generally leads to erratic movements, while immobile and parallel strings are more representative of laminar flows. This test was made at ventilation speeds close to 1 m/s, 2 m/s and 3 m/s for the two tunnels. It led to strings that remained parallel and immobile to the flow direction for the laminar tunnel, while some oscillations were noticed in the case of the turbulent tunnel. Based on these observations both tunnels seem to respond as designed.

The air velocity was also checked in the wind tunnels. The measurements were made using a digital anemometer (Delta Ohm HD2103.1) for velocities around 1 m/s, 2 m/s and 3 m/s for the turbulent tunnel and for velocities around 0.5 m/s, 1 m/s, 1.5 m/s, 2 m/

s and 3 m/s for the laminar tunnel. Results are reported in the Fig. 6.

In the turbulent tunnel, the air velocity gradually increased with the distance from the contraction. Whatever the condition, the difference in velocity between the cup 3 and the cup 1 divided by the mean velocity value led to a relative difference of 8%, which was considered as acceptable.

In the laminar tunnel, a constant air velocity was measured regardless of the position of the measurement (relative difference lower than 3%).

Lastly, the influence of the position of the cup within the tunnels was checked. For that purpose, water vapour permeability tests were realised under unfavourable conditions. Sand samples with a vapor resistance factor close to 1 were tested under the lower ventilation speed in the laminar and turbulent tunnels. This choice of material was motivated by the ease of making identical samples, more permeable than the plasters studied. This experiment led to identical mass variations, whatever the cup position in each tunnel, allowing to deem there is no significant impact on the obtained results.

Table 2 Calculated Reynolds number for different air velocities

	1 m/s	2 m/s	3 m/s
Reynolds	4777	9554	14,331

4 Results and discussion

4.1 Influence of the surface film resistance

A first water vapour resistance factor, denoted by μ , was calculated based on results of vapour permeability

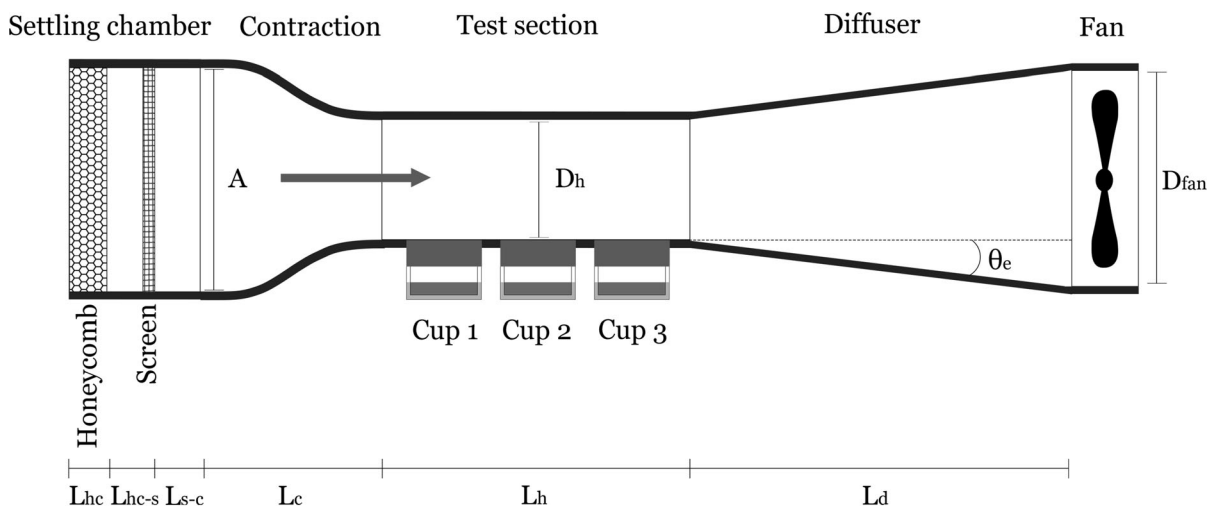
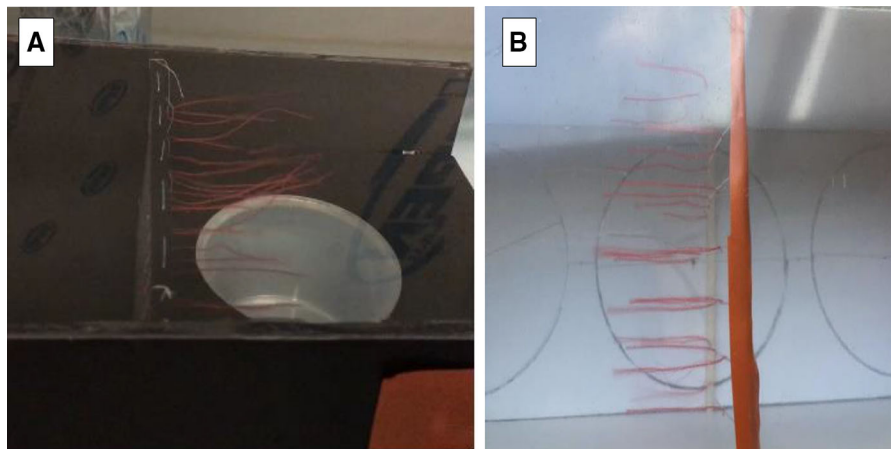


Fig. 4 Schematic representation of the laminar mini-wind tunnel



Table 3 Laminar wind tunnel main characteristics

Component	Symbol	Value	Description	Condition
Test chamber	\emptyset_c	7 cm	Cup diameter	
	D_h	8 cm	Hydraulic diameter	$D_h > \emptyset_c + 2\delta$
	L_h	24 cm	Test chamber length	$L_h/D_h \in [0.5; 3]$
Contraction	A	21.5 cm	Side-length inlet cross-section	
	L_c	19 cm	Contraction length	$L_c/A \in [0.667; 1.79]$
	S_{in}^c	462 cm ²	Contraction inlet section	$S_{in}^c = A^2$; $S_{out}^c = D_h^2$
	S_{out}^c	64 cm ²	Contraction outlet section	$S_{in}^c/S_{out}^c \in [6; 10]$
Fan	D_{fan}	11.5 cm	Fan diameter	
	S_{fan}	132 cm ²	Fan cross-section area	
Diffuser	S_{in}^d	64 cm ²	Diffuser inlet section	$S_{in}^d = D_h^2$; $S_{out} \approx S_{fan}$
	S_{out}^d	132 cm ²	Diffuser outlet section	$S_{out}^d/S_{in}^d \in [6; 10]$
	L_d	24 cm	Diffuser length	
	θ_e	4.2°	Cone expansion angle	$\theta_e < 6^\circ$
Honeycomb	β_h	0.84	Honeycomb open-area ratio	$\beta_h > 0.8$
	D_{hc}	0.6 cm	Honeycomb cell hydraulic diameter	
	L_{hc}	4 cm	Honeycomb cell length	$L_{hc}/D_{hc} \in [6; 8]$
Screen	β_s	0.7	Screens open-area ratio	$\beta_s \in [0.58; 0.8]$
	L_{s-c}	4.5 cm	Distance between screen and contraction	$L_{s-c} \approx 0.2 A$
	L_{s-hc}	20 cm	Distance between screen and honeycomb	$L_{s-hc}/D_{hc} \in [32; 200]$ $L_{s-hc}/L_{hc} \in [4.5; 28]$

**Fig. 5** Experimental visualisation of the flow regime with the tuft test in the **A** turbulent and **B** laminar wind tunnels

using the following expression, which considers only the correction due to the resistance of the air layer in the cup:

$$\mu = \frac{\delta_a}{\delta_p^{ISO}} \quad (10)$$

where δ_a is the water vapour permeability of air and δ_p^{ISO} is the water vapour permeability of the material

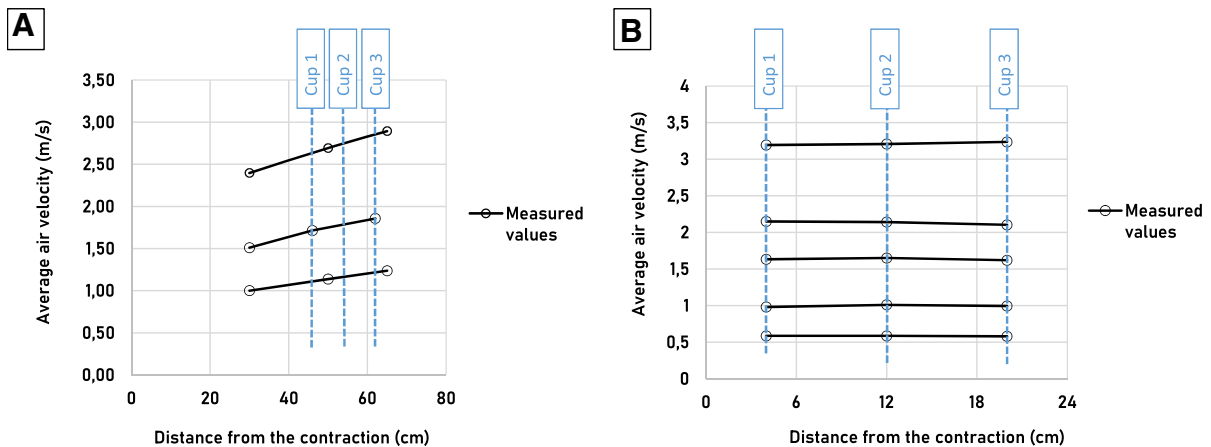


Fig. 6 Measured air velocity in the turbulent (A) and laminar (B) tunnel. The position of the cups are denoted by the vertical dashed lines

defined by the Eq. 6. For clarity, μ_c will be the water vapour resistance based on fully corrected values of the material water vapour permeability :

$$\mu_c = \frac{\delta_a}{\delta_{p,c}}$$

where $\delta_{p,c}$ is the corrected vapour permeability defined by the Eq. (5). In the following of this paper, μ will be designated as “ISO corrected resistance factor”, while μ_c will be called the “corrected resistance factor”.

All measurements realised on earth plaster samples under variable convective conditions showed similar variation of μ . An example is given in Fig. 7 for the sample A9, for most flow regime and air velocity there is a decrease of μ with the thickness of the material. The variation with the thickness of the material is a typical result and has been discussed in several previous papers [21, 22], applying the corrections described in section 2.4.2 allows overcoming this issue and seems to give more robust results based on previous studies [22]. This variation due to the thickness appears in all conditions, yet it seems to be less important at 3 m/s in turbulent and laminar flow. For the same sample, corrected values (μ_c), shown in Fig. 7, are more stable regardless of the flow regime or the air velocity.

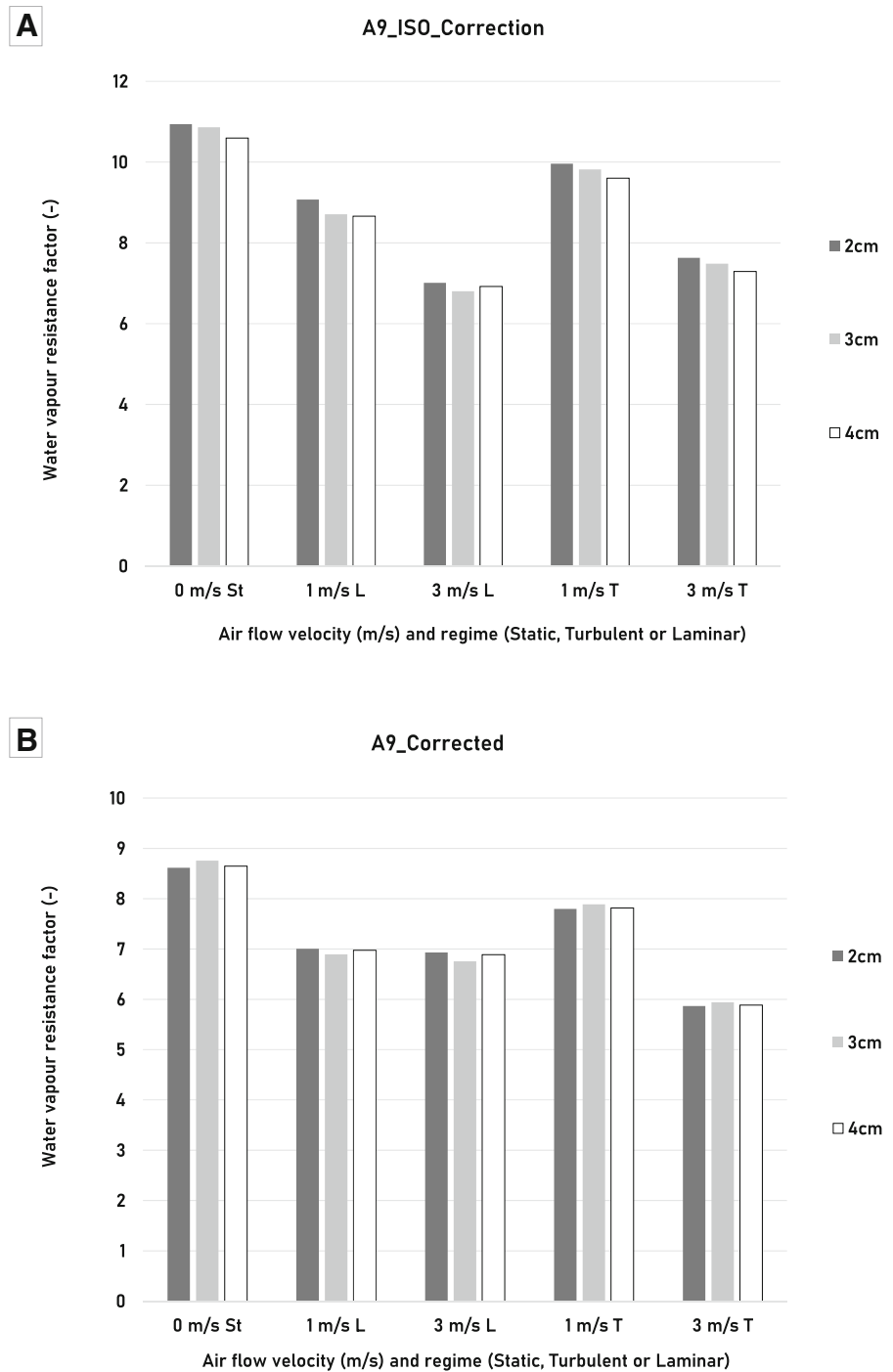
Similar results were found with the other samples. In particular, results of the ISO corrected resistance factor (μ) for an air velocity of 3 m/s in turbulent and laminar flow for each sample are shown in the Fig. 8. The first observation that can be made is that, even when the flow regime is efficiently maintained above

2 m/s as recommended by the standard, the impact of the thickness and therefore the surface film resistance, is still visible. In some cases, the difference between laminar and turbulent flow can be considerable, this is the case for samples A3 and B3. No evident explanation of this difference based on the nature of the materials could be found. This could be however further investigated using additional measurements such as surface roughness. Indeed, surface roughness may accentuate the influence of the surface film resistance and therefore the impact of flow regime and velocity. Those measures were done in the same laboratory and with the same operator, an even greater variation can be expected when measuring in different laboratories, as it was previously noticed by [18].

To analyse further these results, the standard deviation of the measured μ and μ_c on all samples (i.e. on the basis of 36 values per formulation) is given in Table 4. When only the correction due to the resistance of the air layer in the cup is applied, the standard deviation represents between 12 to 30% of the mean value. Once the surface film correction is applied a significant drop of the standard deviation is observed (about 50% in average).

To conclude, those results suggests that even with air velocities higher than the recommended 2 m/s by the standard, the influence of the exterior surface film resistance is not completely cancelled out, and that the surface correction must be applied in order to reach reliable results.

Fig. 7 μ (A) and μ_c (B) values obtained for different air velocities and flow regimes of the A9 sample (St, static; L, laminar; T, turbulent)



4.2 Validation of the surface film correction

While surface parameters will undoubtedly influence the apparent water vapour permeability of the tested material, intrinsic material parameters will certainly

have a primary role on it. Then, looking at the corrected and ISO corrected water vapour resistance factors along an intrinsic material parameter as the density may help to understand the consistency of its values measured under variable conditions. Indeed, it

Fig. 8 ISO corrected water vapour resistance factor (μ) variation with thickness for all samples in a turbulent (T) and a laminar (L) flow with an air velocity of 3 m/s

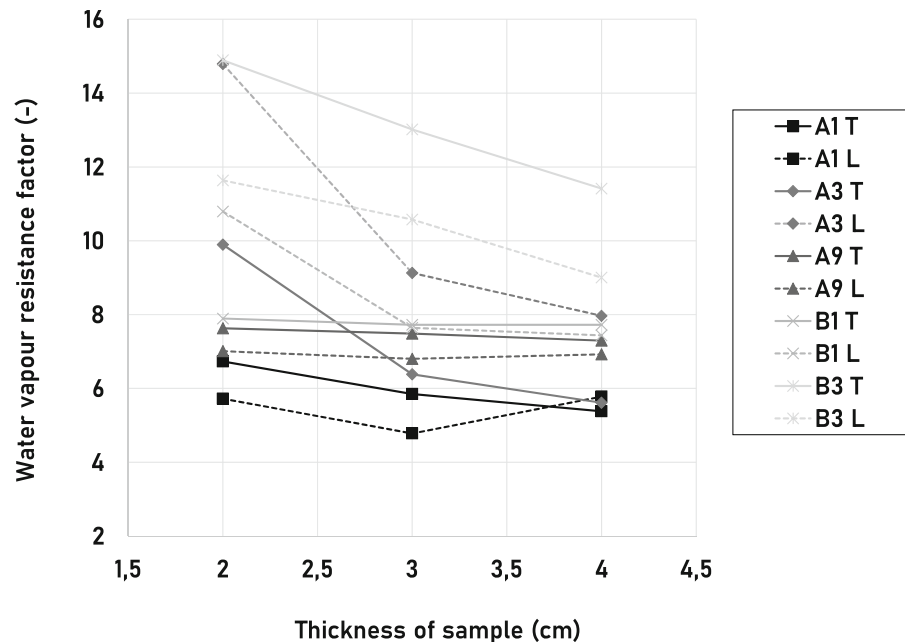


Table 4 Mean value and standard deviation of μ and μ_c

Sample	Uncorrected		ISO corrected		Corrected	
	Mean	SD	Mean	SD	Mean	SD
A1	7.5	1.3	6.4	1.5	5.1	0.6
A3	9.0	2.3	7	1.6	4.1	0.4
A9	10.2	0.6	8.7	0.2	7.2	0.1
B1	10.0	1.2	8.1	0.6	6.7	0.2
B3	14.0	2.1	11.9	1.5	9.2	0.7

is known that, if materials particle size distributions present little variation, the water vapour resistance would tend to increase with density, notably thanks to the decrease in porosity [7]. For this analysis, test conditions and operator for each sample are the same. Furthermore, every sample is made of the same earth. Therefore, the only modified parameters are the earth/sand ratio and the sand particle size. In particular, density was found to increase with the sand to earth ratio.

With this aim in mind, Figs. 9 and 10 compare the water vapour resistance factor based on the standard μ and the factor with correction μ_c in function of the density for every sample, in turbulent and laminar flow. The results show that in laminar as in turbulent

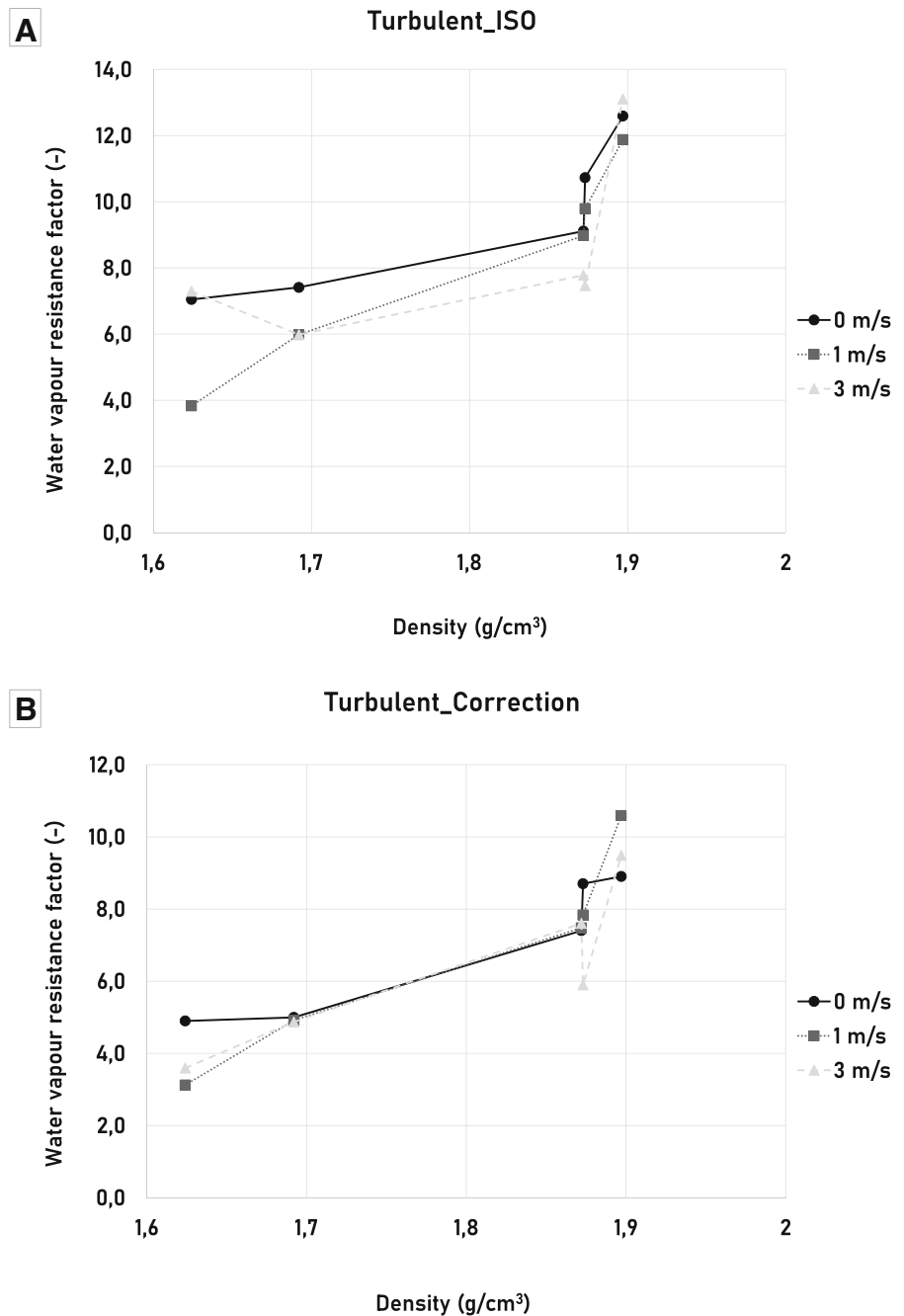
flow, the factor μ presents greater discrepancies with velocity for a same material (each density represents one formulation) and its variation with density does not seem to follow any clear trend. On the other hand, in the case of the corrected coefficient, μ_c , and in particular for turbulent flow regimes, discrepancies due to air velocity are reduced and a global increase of μ_c with the density seems to take shape. Therefore, a more logical phenomenon is observed, and the interest of this surface correction when a material of the same nature under the same conditions is tested can be pointed out.

4.3 Variation of the surface film resistance

While the previous section has demonstrated the influence of the surface film resistance, this section is looking at the numerical values of the film resistance and its variation in different flow regimes. The variation of the surface film resistance is graphically represented in Fig. 11 for turbulent and laminar flow. At first, the obtained values are close to those found in the literature. For example, in [22] water vapour resistance factors were discussed and values of the same order of magnitude, between $6.53 \cdot 10^7$ and $5.57 \cdot 10^8 \text{ m}^2 \text{ s Pa/kg}$, were found for earth plasters.

However, contrary to what would be expected, no straightforward correlation between surface film

Fig. 9 μ (A) and μ_c (B) along the density for different speeds under turbulent flow



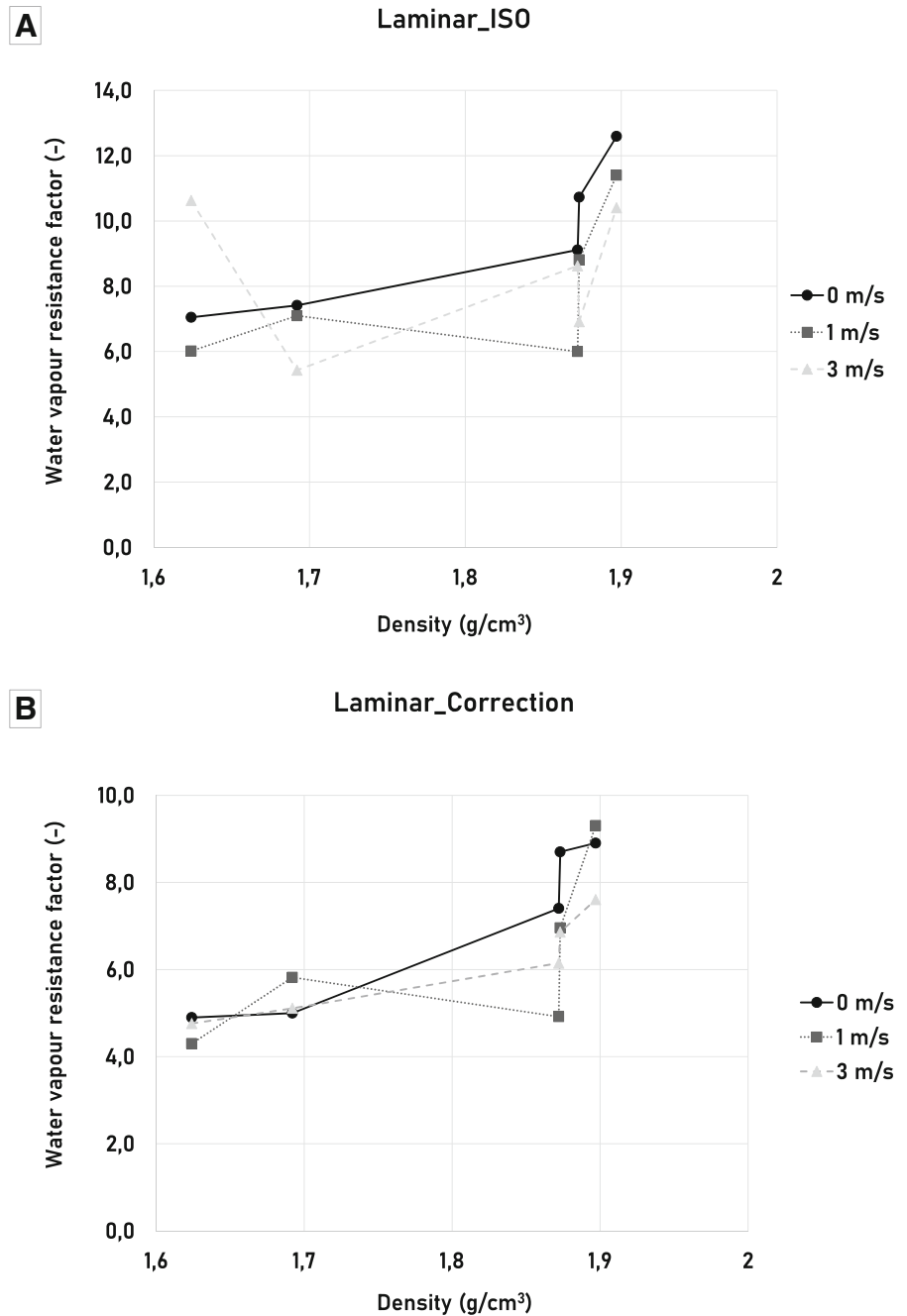
resistance and air velocity emerges. A more erratic behaviour is expected in a turbulent flow, it can be however observed that the values are slightly less dispersed than in the laminar flow. In the turbulent flow, three samples (A1, B1 and A9) actually show a decrease with air velocity which is an expected

behaviour, while the two others show a more erratic evolution.

Values for the laminar flow do not seem to be influenced by air velocity, but they present larger differences between the formulations which were tested, from around $1.10^8 \text{ m}^2 \text{ s Pa/kg}$ for B3 and up to $4.5.10^8 \text{ m}^2 \text{ s Pa/kg}$ for A3. One explanation that



Fig. 10 μ (A) and μ_c (B) along the density for different speeds under laminar flow



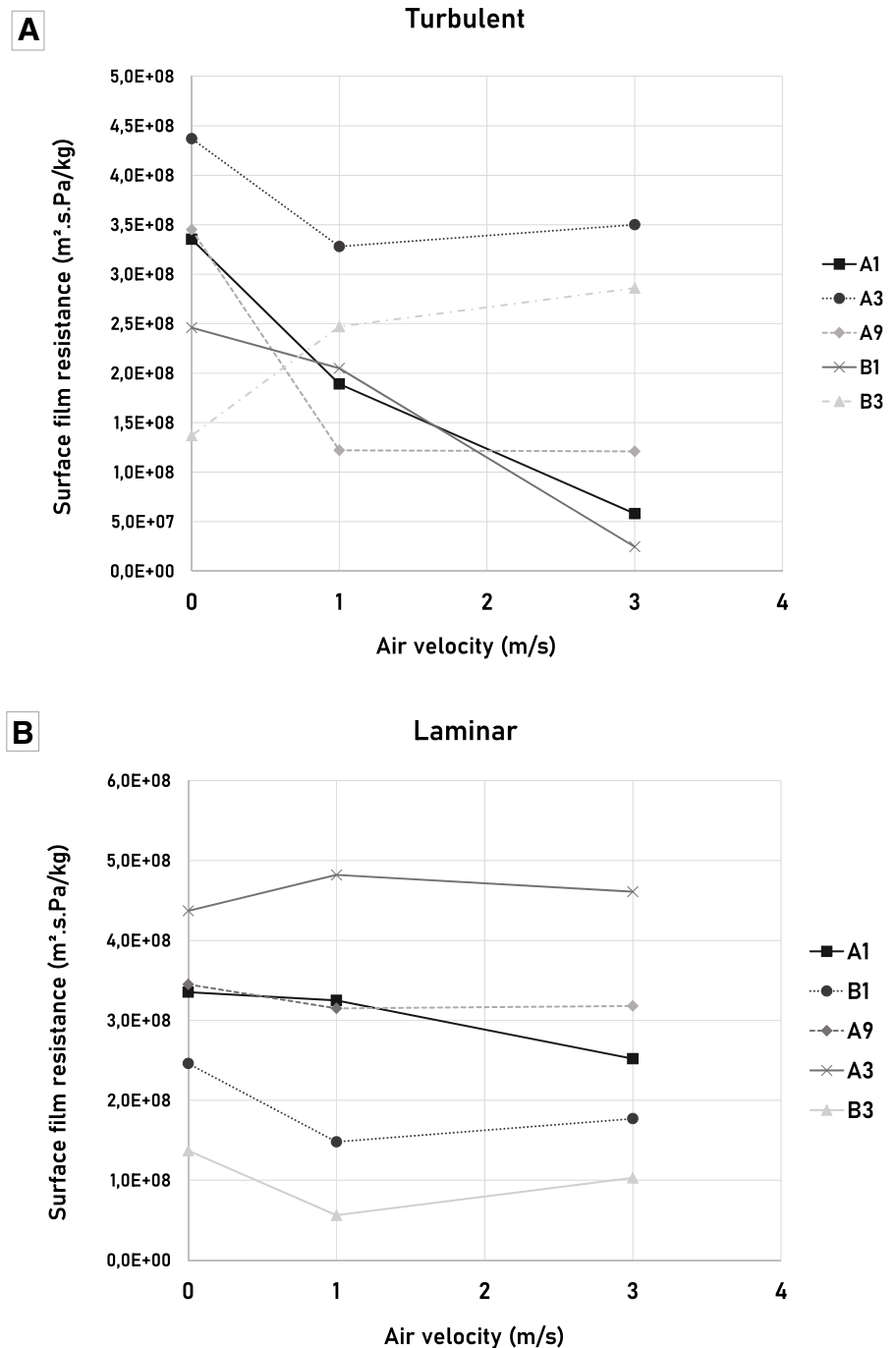
would be worth testing may be sample surface parameters (topography for example), since this latter is known to be influenced by both earth to sand ratio and sand particles size distribution [25].

As it was mentioned in the introduction of this paper, wet and dry cup tests suffer from a poor reliability due to the influence of variable convective

conditions above the cup. In this study, results suggest that increasing the air velocity decreases the surface film resistance in turbulent conditions, while it remains stable in laminar conditions. However, both conditions would still need the application of the correction of the surface film resistance to yield acceptable results. From our results, the influence of



Fig. 11 Variation of the surface film resistance ($Z_s = 1/\beta$) with air velocity in a turbulent (A) and laminar (B) flows



the convective conditions could be examined. It should be notified however that due to the larger number of samples and conditions tested, the replication of series was not applied. To overcome this limitation a verification was done on the mass variation of three identical sand samples, which

showed a perfect correlation. The sand sample can be considered as an ideal replicate, yet the fabrication of the earth plaster samples was also done with great care in the laboratory, reducing the need of replicates due to material heterogeneity. The use of replicates is obviously recommended for non laboratory fabricated

materials to improve the robustness of the measured vapour permeability.

5 Conclusion

In this study, the influence of the air velocity and flow regime on the measurement of the water vapour permeability of earth plasters was investigated. Wind tunnels were specifically designed to correspond to the dimensions of the cups used and to provide either laminar or turbulent flow regimes. The fans used allowed to modify the air velocity above the cups. The wet cup test method was used to determine the water vapour resistance of earth plaster samples under variable convective conditions. Several thicknesses of plasters allowed to determine the surface film resistance at the surface of the earth plasters. The results showed that whatever the flow regime or the air velocity, the surface film resistance should not be neglected in order to assess the water vapour permeability of earth plasters. This means that for highly permeable materials the measures should always be done on 3 different thicknesses of the same material. Taking into account the surface resistance allows reducing at least by half the measured standard deviations. The realisation of this correction has a significant impact on values, since it leads to a reduction of the effective water vapour permeability of the tested samples about 30% and up to 50%. Finally, comparing the corrected water vapour permeability with the density of the material, which is an intrinsic material property, also gives further confidence on the values. Another important outcome is that the surface film resistance appears to strongly depend on the air velocity in turbulent flow regime, while it was found quite stable for a given formulation in laminar flow regime. To conclude, the use of wind tunnels, whether providing laminar or turbulent air flow, may need to be considered in order to achieve more repeatable measures from the water vapour permeability test. In particular, a turbulent wind tunnel which enables to apply a controlled air velocity above the cups was found to lead to accurate and repeatable results. In usual test conditions, such as climatic chambers, the air velocity is not constant nor homogeneous, this may explain the large discrepancies observed in round-robin campaigns. Conversely, the use of a laminar wind tunnel should be preferred for

substantial test campaigns. As the surface film resistance doesn't seem to depend on the air flow velocity, the laminar flow may be more relevant when a precise control of air speed might be complex to achieve.

Declarations

Conflict of interests The authors have no relevant financial or non-financial interests to disclose.

References

1. Morel JC et al (2001) Building houses with local materials: means to drastically reduce the environmental impact of construction. *Build Environ* 36(10):1119–1126
2. Habert G et al (2020) Environmental impacts and decarbonization strategies in the cement and concrete industries. *Nat Rev Earth Environ* 1(11):559–573. <https://doi.org/10.1038/s43017-020-0093-3>
3. Hamard E et al (2018) A new methodology to identify and quantify material resource at a large scale for earth construction: application to cob in Brittany. *Constr Build Mater* 170:485–497. <https://doi.org/10.1016/j.conbuildmat.2018.03.097>
4. Morel JC, Pkla A, Walker P (2007) Compressive strength testing of compressed earth blocks. *Constr Build Mater* 21:303–309
5. Champire F et al (2016) Impact of relative humidity on the mechanical behavior of compacted earth as a building material. *Constr Build Mater*. <https://doi.org/10.1016/j.conbuildmat.2016.01.027>
6. Zhang L et al (2017) Thermal conductivity of cement stabilized earth blocks. *Constr Build Mater* 151:504–511. <https://doi.org/10.1016/j.conbuildmat.2017.06.297047>
7. McGregor F et al (2014) The moisture buffering capacity of unfired clay masonry. *Build Environ*. <https://doi.org/10.1016/j.buildenv.2014.09.027>
8. Hall MR, Casey S (2012) 2-Hygrothermal behaviour and occupant comfort in modern earth buildings. In: Hall MR, Lindsay R, Krayenhoff M (eds) *Modern earth buildings*, Woodhead Publishing series in energy, Woodhead Publishing, pp 17–40. ISBN: 978-0-85709-026-3. <https://doi.org/10.1533/9780857096166.1.17>. <https://www.sciencedirect.com/science/article/pii/B9780857090263500022> (visited on 09/23/2021)
9. McGregor F et al (2016) A review on the buffering capacity of earth building materials. In: *Proceedings of institution of civil engineers: construction materials*, vol 169, no 5. <https://doi.org/10.1680/jcoma.15.00035>
10. Woloszyn M et al (2009) The effect of combining a relative-humidity-sensitive ventilation system with the moisture-buffering capacity of materials on indoor climate and energy efficiency of buildings. *Build Environ* 44(3):515–524. <https://doi.org/10.1016/j.buildenv.2008.04.017>
11. Zhang L, Sang G, Han W (2020) Effect of hygrothermal behaviour of earth brick on indoor environment in a desert



- climate. *Sustain Cities Soc* 55:102070. <https://doi.org/10.1016/j.scs.2020.102070>
12. Colinart T et al (2020) Hygrothermal properties of light-earth building materials. *J Build Eng* 29:101134. <https://doi.org/10.1016/j.jobbe.2019.101134>
 13. Soudani L et al (2017) Energy evaluation of rammed earth walls using long term in-situ measurements. In: *Solar energy*, pp 70–80
 14. Lelievre D, Colinart T, Glouannec P (2014) Hygrothermal behavior of bio-based building materials including hysteresis effects: experimental and numerical analyses. *Energy Build* 84:617–627. <https://doi.org/10.1016/j.enbuild.2014.09.013>
 15. Sereďyński M et al (2020) Analysis of Non-Equilibrium and Equilibrium Models of Heat and Moisture Transfer in a Wet Porous Building Material. *Energies* 13(1):214. <https://doi.org/10.3390/en13010214>
 16. Bui R et al (2020) Uncertainty and sensitivity analysis applied to a rammed earth wall: evaluation of the discrepancies between experimental and numerical data. In: *E3S web of conferences*, vol 172. Publisher: EDP Sciences, p. 17004. ISSN: 2267-1242. <https://doi.org/10.1051/e3sconf/202017217004>. https://www.e3s-conferences.org/articles/e3sconf/abs/2020/32/e3sconf_17004.html (visited on 12/15/2021)
 17. ISO 12572. ISO 12572:2016 Performance hygrothermique des matériaux et produits pour le bâtiment—détermination des propriétés de transmission de la vapeur d'eau - Méthode de la coupelle. In: AFNOR (2016)
 18. Roels S et al (2004) Interlaboratory comparison of hygric properties of porous building materials. *J Therm Envel Build Sci* 27(4):307–325
 19. Feng C et al (2020) Hygric properties of porous building materials (VI): a round robin campaign. *Build Environ*. <https://doi.org/10.1016/j.buildenv.2020.107242>
 20. Pazera M, Salonvaara M (2009) Examination of stability of boundary conditions in water vapor transmission tests. *J Build Phys* 33(1):45–64. <https://doi.org/10.1177/1744259109103228>
 21. Vololonirina O, Perrin B (2016) Inquiries into the measurement of vapour permeability of permeable materials. *Constr Build Mater* 102:338–348. <https://doi.org/10.1016/j.conbuildmat.2015.10.126>
 22. McGregor F et al (2017) Procedure to determine the impact of the surface film resistance on the hygric properties of composite clay/fibre plasters. *Mater Struct*. <https://doi.org/10.1617/s11527-017-1061-3>
 23. Worch A (2004) The behaviour of vapour transfer on building material surfaces: The vapour transfer resistance. *J Thermal Env Build Sci* 28(2):187–200. <https://doi.org/10.3561177/1097196304044398>
 24. Houben H, Guillaud H (2006) *Traite de construction en terre*. Parentheses. <https://www.eyrolles.com/BTP/Livre/traite-de-construction-en-terre-9782863641613/> (visited on 03/05/2021)
 25. Mauffre T et al (2021) Analysis of water droplet penetration in earth plasters using X-ray microtomography. *Constr Build Mater* 283:122651. <https://doi.org/10.1016/j.conbuildmat.2021.122651>
 26. Vololonirina O, Coutand M, Perrin B (2014) Characterization of hygrothermal properties of wood-based products: impact of moisture content and temperature. *Constr Build Mater* 63:223–233. <https://doi.org/10.1016/j.conbuildmat.2014.04.014>
 27. Idelchik IE (1986) *Handbook of hydraulic resistance* (2nd revised and enlarged edition). <https://ui.adsabs.harvard.edu/abs/1986wdch.bookI>
 28. Bell JH, Mehta J (1988) Contraction design for small low-speed wind tunnels. In: NASA report. <https://www.semanticscholar.org/paper/Contraction-Design-for-Small-Low-Speed-Wind-Tunnels-Bell-Mehta/d78fabf4192488181c6642994e868834cfe501e7>
 29. Mauro S (2017) Small-scale open-circuit wind tunnel: design criteria, construction and calibration

Publisher's Note Springer Nature remains neutral with regard to jurisdictional claims in published maps and institutional affiliations.

